Science Journal of Chemistry
2020; 8(5): 124-130
http://www.sciencepublishinggroup.com/j/sjc
doi: 10.11648/j.sjc.20200805.15
ISSN: 2330-0981 (Print); ISSN: 2330-099X (Online)

Infrared Line Collisional Parameters of PH_3 in Hydrogen: Measurements with Second-order Approximation of Perturbation Theory

Jamel Salem*, Rached Ben Younes

Department of Physics, Faculty of Science of Gafsa, University of Gafsa, Gafsa, Tunisia

Email address:
sfjamel1@yahoo.fr (J. Salem), rached_benyounes@yahoo.fr (R. ben Younes)
*Corresponding author

To cite this article:
Jamel Salem, Rached Ben Younes. Infrared Line Collisional Parameters of PH_3 in Hydrogen: Measurements with Second-order Approximation of Perturbation Theory. *Science Journal of Chemistry*. Vol. 8, No. 5, 2020, pp. 124-130. doi: 10.11648/j.sjc.20200805.15

Received: March 24, 2020; **Accepted**: August 24, 2020; **Published**: October 26, 2020

Abstract: Measurement of room temperature absorption by PH_3–H_2 mixtures in the ν_2 and ν_4 bands of phosphine (PH_3) have been made for low pressures. Fits of these spectra are made for the determination of the width for isolated lines, and line mixing in first-order Rosenkranz approximation. From the previous determinations, we deduce some remarks on the lack of accuracy for the prediction of the collisional process. With the first-order Rosenkranz approximation, the collisional parameters are considered linear with pressure. In this work, we have considered some spectra recorded for three doublets A_1 and A_2 lines in the ν_2 and ν_4 bands of PH_3 diluted with higher H_2 pressure. We show that the line shifts are non-linear with perturber pressures, which requires testing the fits of the recorded spectra by profiles developed in the second-order approximation of the perturbation theory. Consequently, the first and second-order mixing coefficients are determined and discussed. Also, through this study, we show that the change of the intensities distribution is provided by the populations exchange between the low energy levels for the two components of doublets A_1 and A_2 lines and is described through the second-order mixing parameter. Thereby, we show the mixing effect on the line width.

Keywords: Phosphine, Hydrogen, Collisional Parameters, Infrared, Second-order Approximation

1. Introduction

Phosphine is a molecule observed in the atmosphere of Jupiter and Saturn [1-4] composed mainly of hydrogen and helium. Also, the study of its broadened spectra by the H_2 pressure can be useful in the modeling of the planetary atmospheres. Therefore, it is of astrophysical interest. In addition, the study of their overlapping lines can give some information on the collisional dynamics of this molecule, as well as on the radiative transfer between relative transitions, which is of fundamental interest.

In order to model a ro-vibrational spectrum, different procedures and approximations have been established to adjust the spectral lines of some molecules in the infrared region. In the framework of the isolated line approximation, the absorption lines of the ν_2 and ν_4 bands of phosphine (PH_3) recorded using a diode-laser spectrometer are fitted with the Voigt, Rautian and speed-dependent Rautian profiles [5-10]. In the framework of first-order Rosenkranz approximation, some experimental spectra of the same ν_2 and ν_4 bands of PH_3 diluted with hydrogen (H_2) at room and low temperatures were analyzed by means of non-linear least-squares multi-pressure fitting procedures based on the collisional Rosenkranz profile [11, 12]. In other works, the ro-vibrational spectra of other molecules like CH_4, NH_3, CH_3Br, C_3H_4 are fitted with the same procedures [13-16].

The collisional line width shows a linear regression with perturber pressure. The same applies to the intensity parameter vs the pressure of the active gas. On the other hand, the line-shift shows in some papers a non-linear variation with the perturber pressure [14, 17, 18], which is incoherent with the hypotheses of the isolated lines and first-order Rosenkranz approximations. In fact, the reconstruction of the collisional profiles is based on the diagonalization of the relaxation matrix as part of the impact approximation. A simple and well-known method of calculation is that of the perturbation theory used in

the construction of the profiles previously mentioned.

Smith [19] extended the first-order Rosenkranz approximation [20] to the second-order in the framework of perturbation theory. His work yields a collisional profile taking into account the first and second-order parameters of the line mixing effects. In this same profile expression, the line-shift has parabolic form vs the perturber pressure.

In this work, we have used the collisional profile expression given by Smith to analyze some spectra of three doublets A_1 and A_2 lines recorded using a diode-laser spectrometer in the ν_2 and ν_4 bands of PH_3 diluted with H_2 at higher pressure and room temperature. Then, we have specified the collisional parameters to adjust. Also, the reconstruction of the recorded spectra justifies the need to take into account of the second order mixing and shifting parameters. As results, the first and second-order H_2-line mixing coefficients in the ν_2 and ν_4 bands of PH_3 are presented and discussed. Also, through this study, we show the line mixing effect on the intensities distribution and widths.

2. Experimental Analysis

2.1. Experimental Conditions

The absorption spectra of PH_3-H_2 mixture in the ν_2 and ν_4 bands of phosphine were recorded at high resolution using a tunable diode-laser spectrometer (Laser Analytics Model LS3). The experimental techniques are detailed in Ref. [21, 22]. We give in this work the experimental conditions of measurements verifying our analysis procedure.

The absorption path length of the IR radiation provided by the diode-laser in the multipass white-type cell is fixed to 20.17 m. The phosphine sample is supplied by Union Carbide with a stated purity of 99.999% and the hydrogen sample is supplied by Air Liquide with a stated purity of 99.99%. The gas pressure was measured by two Baratron MKS gauges with full scale measurements of 1.2 and 120 mbar with an accuracy of 5×10^{-4} and 2×10^{-2} mbar, respectively. All spectra are recorded at room temperature (i.e. 297.2 ±1.5 K). Table 1 summarizes the data needed for the transitions studied in this work: wavenumbers, pressure of PH_3 (P_{PH_3}), Doppler half-width (γ_{Dop}), effective Doppler half-width ($\gamma_{D_{eff}}$), temperature (T) and pressure of H_2 (P_{H_2}). Also, Figure 1 shows an example of the recorded spectra of the doublet ^{R}R (4, 3, A_1) and ^{R}R (4, 3, A_2) lines of the ν_4 band of PH_3 diluted with pressures of H_2, where the transmittance is plotted vs the point numbers. The relative calibration of spectra was performed using a confocal etalon with an interfringe spacing was of 0.007958 cm^{-1}. The etalon fringe pattern provided a check of the laser mode quality for correction of the slightly nonlinear tuning of the diode-laser. Furthermore, it aided in linearization of the spectra with a constant step of 0.000121 cm^{-1}. All spectra were linearized using the cubic splines techniques [24].

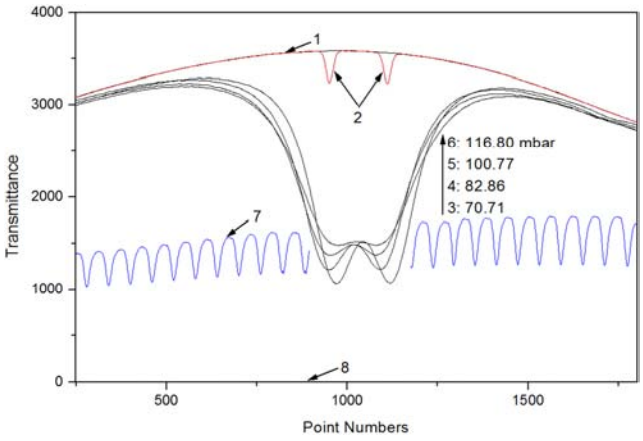

Figure 1. *Examples of the recorded spectra for the A_1A_2 components of the ^{R}R (4, 3) doublet transition in the ν_4 band of PH_3 diluted by H_2. (1) Baseline recorded with empty cell, (2) Effective Doppler lines recorded at low-pressure of pure PH_3: 0.029 mbar, (3-6) records of the broadened at different pressures of H_2: 70.71, 82.86, 100.77 and 116.80 mbar, (7) confocal etalon fringes pattern, (8) 0% transmission level.*

Table 1. *Experimental conditions of the recorded spectra.*

Transition	Wavenumber $\sigma(cm^{-1})$ [23]	P_{PH_3} $(mbar)$	γ_{Dop} $(10^{-3}cm^{-1})$	$\gamma_{D_{eff}}$ $(10^{-3}cm^{-1})$	T (°K)	P_{H_2} $(mbar)$
ν_2 band						
^{Q}R (8, 3, A_1)	1059.14042	0.0010	1.1248	1.1484	298.15	55.14, 65.88, 80.70, 102.29
^{Q}R (8, 3, A_2)	1059.14988			1.1473		$P_{PH_3} = 0.022\ mbar$
^{Q}R (9, 3, A_1)	1065.05928	0.0009	1.1299	1.2220	297.65	59.13, 72.86, 86.15, 111.20
^{Q}R (9, 3, A_2)	1065.07558			1.2039		$P_{PH_3} = 0.021\ mbar$
ν_4 band						
^{R}R (4, 3, A_1)	1174.62613	0.0009	1.2466	1.3454	297.75	70.71, 82.86, 100.77, 116.80
^{R}R (4, 3, A_2)	1174.64546			1.3464		$P_{PH_3} = 0.029\ mbar$

2.2. Profiles and Fitting Procedure

The spectra recorded using the diode-laser spectrometer allow to write the Beer-Lambert law,

$$\alpha(\sigma) = \frac{1}{l} Ln[\frac{I_0(\sigma)}{I_t(\sigma)}]. \quad (1)$$

$\alpha(\sigma)$ is the experimental absorbance per unit length at wavenumber σ in cm^{-1}, l is the path length, $I_0(\sigma)$ and $I_t(\sigma)$ are the transmitted intensities measured with the cell under vacuum and filled with the gas sample, respectively.

To fit the recorded spectra, three physical effects must be taken into account: the weak instrumental distortion, the Doppler and collisional effects. The first is implicitly taken into account through the effective half-width $\gamma_{D_{eff}}$ obtained by fitting the effective Doppler line [25] (see Table 1). The Voigt profile (VP) results from the convolution of the Doppler and collisional profiles reflecting the latter two effects. The expression of this profile depends on the extension of the collisional profile to be considered.

Considering the collisional profile proposed by Smith [19]

and developed within the framework of the second-order approximation of perturbation theory:

$$\alpha_C(\sigma) = \frac{P_{PH3}}{\pi}\sum_{line\ k} S_k \left[\frac{\gamma_k(1+P^2 g_k)+(\sigma-\sigma_k+P^2\delta\sigma_k)PY_k}{(\sigma-\sigma_k+P^2\delta\sigma_k)^2+(\gamma_k)^2}\right], \quad (2)$$

where the index k represent transitions in Liouville or "line" space, S_k , γ_k and Y_k are respectively the coupled line strength, the collisional half-width and the first-order line mixing coefficient. The wavenumber $\sigma_k = \sigma_{0k} - \delta_k$, where σ_{0k} is the line center wavenumber and δ_k is the line-shift. g_k, it's the second-order line-mixing coefficient and $\delta\sigma_k$ it's the second-order line-shift coefficient.

In this paper, we deduce the Voigt profile (VPI2) corresponding to this collisional profile as:

$$\alpha_{VPI2}(\sigma) = \frac{P_{PH3}}{\gamma_{Deff}\sqrt{\pi}}\sum_{line\ k} S_k.\{(1+P^2 g_k).Re[W(x,y)] + PY_k.Im[W(x,y)]\}, \quad (3)$$

where $W(x,y)$ is the complex probability function expressed by [26]:

$$W(x,y) = \left(\frac{i}{\pi}\right)\int_{-\infty}^{+\infty}\frac{e^{-t^2}}{x-t+iy}dt, \quad (4)$$

where $x = \sqrt{Ln2}(\sigma - \sigma_k + P^2\delta\sigma_k)/\gamma_{D_{eff}}$ and $y = \sqrt{Ln2}\,\gamma_k/\gamma_{D_{eff}}$.

It should be noted that $\sigma_k, P^2\delta\sigma_k, \gamma_k, PY_k$ and $P^2 g_k$ parameters are related to the diagonal (W_{kk}) and off-diagonal ($W_{kk'}$ with $k' \neq k$) elements of the collisional relaxation matrix (W) [19]. If the second-order parameters ($\delta\sigma_k$ and g_k) equals to zero, then Equation (3) reduce to the expression of first-order Rosenkranz approximation model (VPI1) [18, 27].

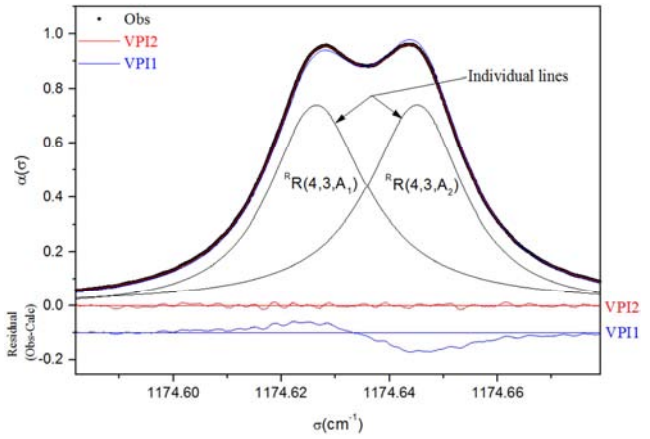

Figure 2. *The measured profile for the A_1A_2 components of the ^{R}R (4, 3) doublet transition in the ν_4 band of PH_3 diluted by 100.77 mbar of H_2 (•), and fitted superposed theoretical profiles: VPI2 (—), and VPI1 (—). The deviations from the fits (Obs-Calc) residuals: from VPI2 (—), and from VPI1 (—). The (Obs-Calc) residuals are multiplied by 5 and displaced vertically for visibility.*

To fit the observed spectra, we have set the intensity parameter to the value deduced from the absolute line intensity of Ref. [18]. Figure 2 shows an example of the fits for the A_1 and A_2 lines of the doublet ^{R}R (4, 3) in the ν_4 band of PH_3 diluted with 100.77 mbar of H_2 by theoretical profiles: VPI1 and VPI2. The (Obs-Calc) residuals are multiplied by 5 and displaced vertically for visibility. The (Obs-Calc) residuals of VPI2 show a better reproduction of the observed lines than that given by VPI1 were the second-order line mixing parameter is not taken into account. The better reconstruction given by VPI2 mainly reflects the contribution of the second-order mixing parameter to the reproduction of the lines at the peak.

3. Results and Discussion

3.1. Line Intensities

Using the absolute line intensities $S_0(10^{-3}\ cm^{-2}atm^{-1})$ of Ref. [18], the absorption path length l and the constant partial pressure of PH_3 (P_{PH_3}) in the gas mixtures, we have deduced the intensity parameter $S(10^{-3}cm^{-1})$ for each studied transition. This parameter is fixed in the used fit profiles for all four recorded spectra broadened by four different H_2 pressures. Consequently, we can fit the first and second-order line mixing parameters (respectively, PY and P^2g). This idea allows us to distinguish the proper line intensity from the rate of intensity transferred with the neighboring line during the overlap.

Figure 3 gives qualitative examples showing the difference between: the intensities distribution in two overlapping lines: $S(1+P^2g)$ obtained in this work, and the line intensities presented with their errors ($S \pm \Delta S$) deduced from the results of Ref. [18]. These examples are presented for the A_1 and A_2 lines of the doublets ^{Q}R (8, 3) in the ν_2 band and ^{R}R (4, 3) in the ν_4 band of PH_3 vs the square of the pressure of hydrogen $P^2(in\ atm^2)$.

Table 2. *Measured line intensities for the A_1A_2 components of the doublets transition in the ν_2 and ν_4 bands of PH_3 with theirs estimated errors.*

Transition	Wavenumber $\sigma(cm^{-1})$ [23]	Line Intensity $(10^{-3}cm^{-1})$ $(S \pm \Delta S)$: [18]	S': [28]	$S(1+P^2g)$: This Work	Diff (%)
ν_2 band					
^{Q}R (8, 3, A_1)	1059.14042	21.656 ± 0.433	21.678	22.311 → 23.127	2.92 ~ 6.68
^{Q}R (8, 3, A_2)	1059.14988	21.831 ± 0.438	21.590	21.064 → 20.471	2.43 ~ 5.18
^{Q}R (9, 3, A_1)	1065.05928	16.570 ± 0.330	16.470	16.535 → 16.667	0.39 ~ 1.20
^{Q}R (9, 3, A_2)	1065.07558	16.483 ± 0.330	16.470	16.488 → 16.280	0.11 ~ 1.15
ν_4 band					
^{R}R (4, 3, A_1)	1174.62613	27.317 ± 0.548	27.317[a]	27.700 → 28.319	1.40 ~ 3.67
^{R}R (4, 3, A_2)	1174.64546	27.311 ± 0.548	27.363	27.175 → 26.407	0.69 ~ 3.49

a: This value is that of Ref. [18].

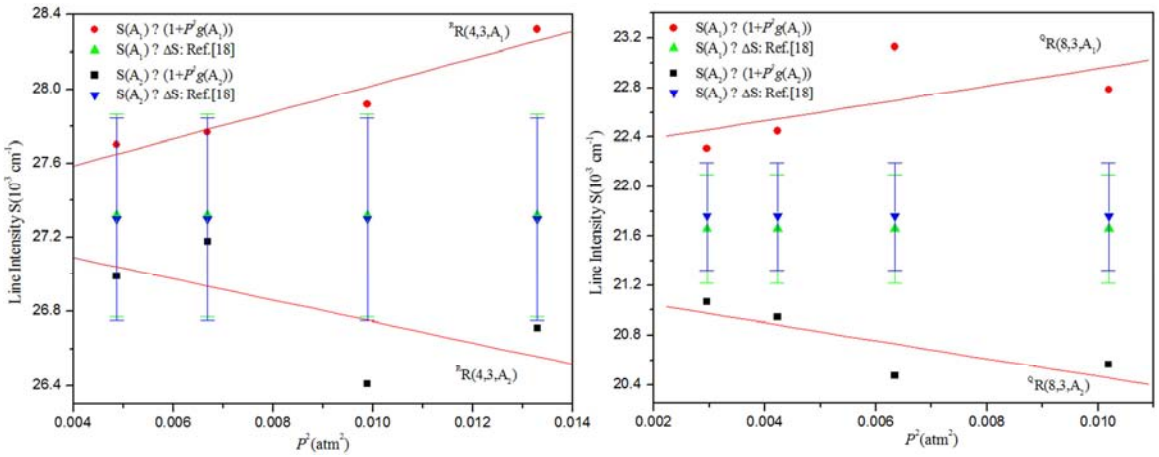

Figure 3. *Qualitative examples showing the difference between: the intensities distribution in two overlapping lines: $S(1 + P^2 g)$ obtained in this work, and the line intensities presented with their errors $(S \pm \Delta S)$ deduced from the results of Ref. [18]. These examples are presented for the A_1 and A_2 lines of the doublets ^{Q}R (8, 3) in the ν_2 band and ^{R}R (4, 3) in the ν_4 band of PH_3 vs the square of the pressure of hydrogen $P^2(in\ atm^2)$.*

From Figure 3, we observed almost linear variation of the intensities distribution between the two overlapping A_1 and A_2 lines vs P^2. The slopes of the straight lines of these variations have opposite signs. Table 2 shows that the variation of the intensities distribution obtained by this work exceeds sometimes the measurement uncertainties of the line intensities. Also, they differ from Brown's measurements [28] by a that can reach 6.68% in the case of the line ^{Q}R (8, 3, A_1).

3.2. Broadening Coefficients and Line Mixing Effects

Figure 4 shows a typical linear regression on the values of the collisional half-width measured at each of the four pressures of H_2 for the ^{R}R (4, 3) doublet A_1 and A_2 lines of PH_3. The collisional half-widths are measured using the VPI2 profile. The slopes of the straight lines correspond to the H_2-broadening coefficients $\gamma_0(in\ 10^{-3} cm^{-1} atm^{-1})$. Here, we have systematically considered the small self-broadening contributions (represented by a point close to the origin) derived from the self-broadening coefficients calculated using the theoretical model detailed in Ref. [6], and from the constant partial pressure of PH_3 in the gas mixtures. The measurements of γ_0 are presented in Table 3 with their errors given by the standard deviation derived from the linear least-squares fit. The average values of the broadening coefficients of the A_1 and A_2 lines are in good agreement with these obtained in Ref. [18] where the second-order mixing parameter is neglected. But any appreciable difference between these coefficients of each line is shown on percent in Table 3. This behavior reflects the line mixing effect on the line widths and it's shown by the fact of taking into account of the second-order mixing term given by Smith's development. In same branch, the line mixing effect on the width decrease with the rotational quantum number J ie, when the difference wavenumber $\Delta\sigma$ increases (see Table 3).

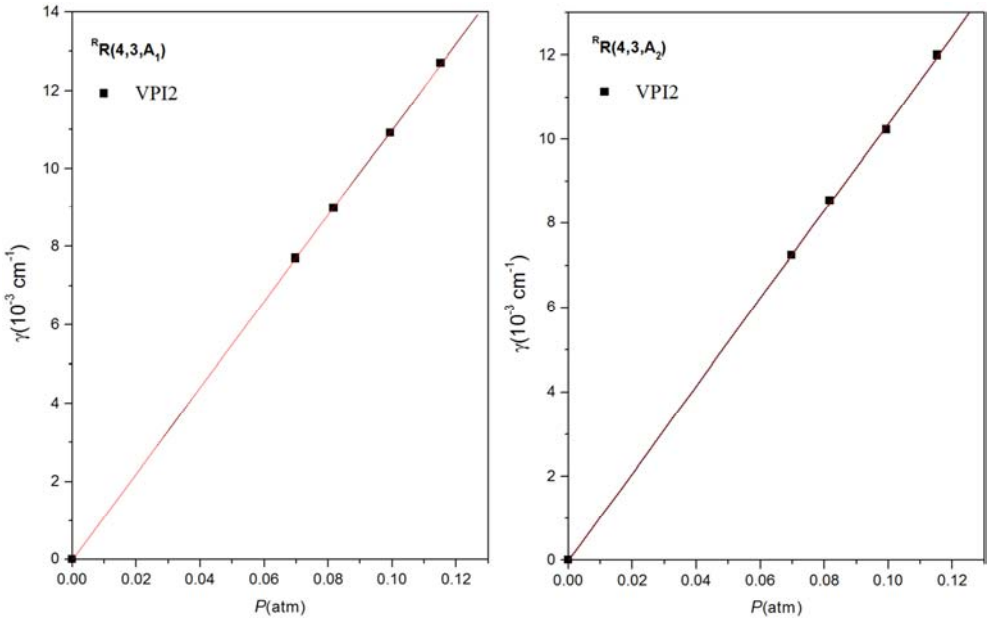

Figure 4. *Linear regression of the collisional width γ for the ^{R}R (4, 3) doublet A_1 and A_2 lines in the ν_4 band of PH_3, derived from the fit of VPI2 (•). The point close to the origin represents the self-broadening contribution.*

Table 3. *Measured H_2-broadening coefficients for the A_1A_2 components of the doublets transition in the ν_2 and ν_4 bands of PH_3 with theirs estimated errors.*

Transition	Wavenumber $\sigma(cm^{-1})$ [23]	[a]$\Delta\sigma$ (cm^{-1})	$\gamma_0(10^{-3}cm^{-1}atm^{-1})$ VPI2	[b]γ_{0Av}	([c]$\Delta\gamma_0/\gamma_{0Av}$) (%)	Ref. [18]
ν_2 *band*						
^{Q}R (8, 3, A_1)	1059.14042	0.00946	102.27 (1.07)	100.5 (2.6)	3.48	98.01 (0.76)
^{Q}R (8, 3, A_2)	1059.14988		98.77 (0.58)			97.25 (0.55)
^{Q}R (9, 3, A_1)	1065.05928	0.01630	96.34 (1.13)	96.5 (1.1)	0.34	97.31 (0.16)
^{Q}R (9, 3, A_2)	1065.07558		96.67 (0.71)			97.20 (0.53)
ν_4 *band*						
^{R}R (4, 3, A_1)	1174.62613	0.01933	109.97 (0.96)	106.8 (4.8)	5.85	107.15 (0.24)
^{R}R (4, 3, A_2)	1174.64546		103.72 (2.31)			106.83 (0.50)

a $\Delta\sigma(cm^{-1}) = |\sigma(A_1) - \sigma(A_2)|$

b $\gamma_{0Av} = \frac{\gamma_0(A_1)+\gamma_0(A_2)}{2}$

c $\Delta\gamma_0 = |\gamma_0(A_1) - \gamma_0(A_2)|$

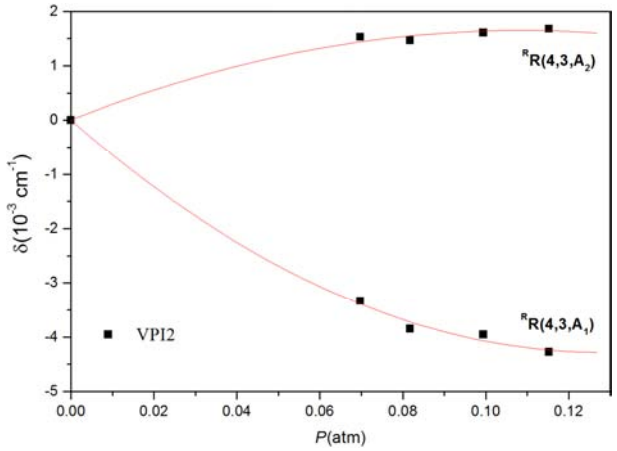

Figure 5. *Pressure dependence of the line shifts δ for the ^{R}R (4, 3) doublet A_1 and A_2 lines in the ν_4 band of PH_3, derived from the fit of VPI2 (•). The point close to the origin represents the self-shifting contribution. The best fit curves represent the second-order polynomial functions whose first and second-order coefficients are respectively, the first and second-order H_2-shifting coefficients for each transition.*

3.3. Line Shifting Parameters

Figure 5 shows a typical plot of the line-shift $\delta(10^{-3}\ cm^{-1})$ derived from the VPI2 profile versus the H_2 pressure $P\ (in\ atm)$ for the ^{R}R (4, 3, A_1) and ^{R}R (4, 3, A_2) lines in the ν_4 band of PH_3. The point close to the origin represents the self-shifting contribution (δ_{self}). The measured values show a quadratic dependence on pressure, that it's coherent with the theoretical analyses given by the development of the second-order perturbation theory of Smith [19]. Consequently, from unconstrained second-order polynomial least-squares procedures we deduce the first and second-order coefficients of the curves, which are the first-order $\delta_0(10^{-3}\ cm^{-1}atm^{-1})$ and second-order $\delta\sigma(10^{-3}\ cm^{-1}atm^{-2})$ H_2-shift coefficients, respectively. Indeed, the line-shift parameter for each line k is expressed in the framework of the development of the second-order perturbation theory as:

$$\delta_k = \delta_{self} + P\delta_{0k} + P^2\delta\sigma_k. \quad (5)$$

Where, the first-order coefficient δ_{0k} is related to the imaginary part of the diagonal (W_{kk}) elements of the collisional relaxation matrix (W), and the second-order coefficient $\delta\sigma_k$ is related to their off-diagonal elements ($W_{kk'}$ with $k' \neq k$) by [19]:

$$\delta\sigma_k = \sum_{k'\neq k} \frac{W_{kk'}W_{k'k}}{\sigma_{0k'} - \sigma_{0k}}. \quad (6)$$

In this work, we restrict to presents a qualitative behavior of the line-shift parameter with the perturber pressure. This behavior is coherent to the hypothesis of the second-order Smith's development.

3.3.1. First-order Line Mixing Parameter

Figure 6 shows two examples of the variation of the fitted first-order line mixing parameter (PY) by VPI2, with H_2 pressure $P(in\ atm)$ for the A_1 and A_2 lines of the ^{R}R (4, 3) doublet in the ν_4 band of PH_3. The first-order H_2-line mixing coefficients $Y(\ in\ 10^{-3}atm^{-1})$ are deduced from the slope of the straight lines resulted from unconstrained linear least-squares procedures. These values obtained with their errors given by the standard deviation on Y derived from the linear least-squares fit are presented in Table 4.

For the components A_1 and A_2 of the doublet lines, the first-order mixing coefficients are opposite. Except the mixing coefficients of ^{Q}R (8, 3) doublet lines where it's underestimated, our results present in this work are in satisfactory agreement with these given by Ref. [18]. In the ^{Q}R branch, the first-order mixing coefficients shows a decrease in absolute value with the rotational quantum number J ie, when the difference wavenumber $\Delta\sigma$ increases (see Table 4).

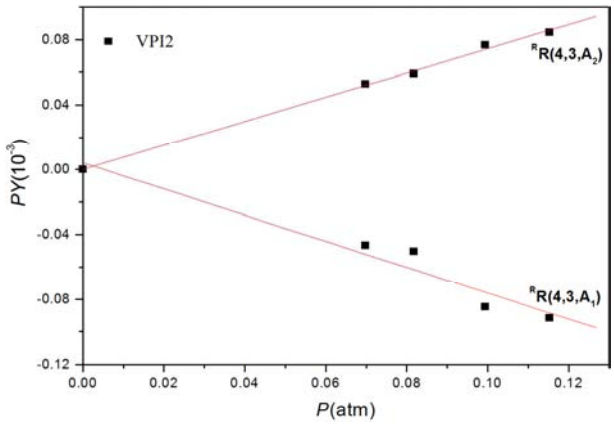

Figure 6. *Pressure dependence of the first-order mixing parameter PY for the A_1A_2 components of the ^{R}R (4, 3) doublet transition in the ν_4 band of PH_3, derived from the fit of VPI2 (•). The slopes of the best-fit lines represent the first-order H_2-line mixing coefficients for each transition.*

Table 4. *First and second-order H_2-line mixing coefficients for the A_1A_2 components of the doublets transition in the ν_2 and ν_4 bands of PH_3 with theirs estimated errors.*

Transition	Wavenumber $\sigma(cm^{-1})$[23]	[a]$\Delta\sigma$ (cm^{-1})	$Y(10^{-3}atm^{-1})$ VPI2	[b]Ref. [18]	$g(10^{-3}atm^{-2})$ VPI2
ν_2 *band*					
^{Q}R (8, 3, A_1)	1059.14042	0.00946	-1.77 (0.16)	-3.23 (0.40)	3.28 (1.74)
^{Q}R (8, 3, A_2)	1059.14988		1.71 (0.27)	3.31 (0.56)	-3.30 (1.05)
^{Q}R (9, 3, A_1)	1065.05928	0.01630	-1.32 (0.04)	-1.47 (0.59)	0.93 (0.15)
^{Q}R (9, 3, A_2)	1065.07558		0.92 (0.44)	0.86 (0.27)	-1.45 (0.30)
ν_4 *band*					
^{R}R (4, 3, A_1)	1174.62613	0.01933	-1.12 (0.23)	-0.92 (0.22)	2.65 (0.27)
^{R}R (4, 3, A_2)	1174.64546		0.74 (0.07)	0.76 (0.43)	-2.09 (0.95)

[a] $\Delta\sigma(cm^{-1}) = |\sigma(A_1) - \sigma(A_2)|$

[b] These values correspond to the average of the measurements obtained with the two models (VP with mixing and SDRP with mixing).

The line mixing (off-diagonal relaxation elements) coefficients (W_{ij}) for the A_1A_2 pairs of transitions in the phosphine pentad given by V. Malathy Devi et al. [29] are seen and compared to mine.

3.3.2. Second-order Line Mixing Parameter

Two typical examples of the variation of the second-order line mixing parameter (P^2g) deduced by fit with VPI2 profile vs the square of the pressure of hydrogen $P^2(in\ atm^2)$ are shown in Figure 7 for the ^{R}R (4, 3) doublet A_1 and A_2 lines in the ν_4 band of PH_3. The second-order H_2-line mixing coefficients $g(in\ 10^{-3}atm^{-2})$ are derived from the slope of the straight lines resulted from unconstrained linear least-squares procedures. These values obtained with their errors given by the standard deviation on g derived from the linear least-squares fit are presented in Table 4.

The measurement uncertainties are less than 31.8% for the studied transitions, except for ^{Q}R (8, 3, A_1) and ^{R}R (4, 3, A_2) lines which are in the range of 53% and 45%, respectively.

For each doublet lines A_1 and A_2, these second-order mixing coefficients are opposite, which reflects the rate of intensity exchange during the overlap due to the transfer of population between low energy levels of the two transitions. With the pressures range considered by this work, the second-order mixing term becomes appreciable and thereafter it is measurable, while at lower pressures it's indistinguishable from the measured uncertainties of line intensities such as the case of the spectra studied in Ref. [18]. Like the observed behavior of the first-order mixing parameter, this last show in the ν_2 band a decrease with the rotational quantum number J, where the difference wavenumber $\Delta\sigma$ increases (see Table 4).

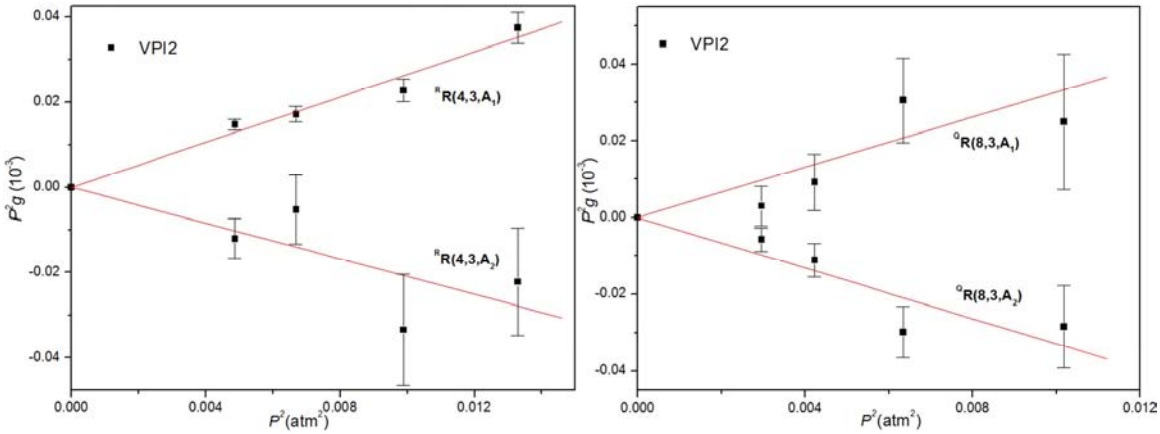

Figure 7. *Variation of the second-order mixing parameter P^2g with their bar error vs the square of the H_2-pressure for the A_1A_2 components of the doublets transition ^{Q}R (8, 3) in the ν_2 band and ^{R}R (4, 3) in the ν_4 band of PH_3, derived from the fit of VPI2 (•). The slopes of the best-fit lines represent the second-order H_2-line mixing coefficients for each transition.*

4. Conclusion

This work presents reasonable first and second-order mixing coefficients within the framework of the second-order approximation of perturbation theory for some lines in the ν_2 and ν_4 bands of PH_3 perturbed by H_2 at room temperature. To achieve these results, we have used the spectra recorded at ranged pressures from 55 to 117 mbar using a diode laser spectrometer. Also, we have considered the collisional profile proposed by Smith [19] and developed within the framework of the second-order perturbation theory. This allows to deduce the VPI2 profile by convolution with the Doppler profile.

The obtained shifting parameter shows a parabolic variation with the perturber pressure, which is justified by the second-order approximation used. We have set the intensity

parameter in the fit profiles; this allows us to distinguish between the appropriate line intensity and the intensity rate exchanged with the neighboring line during the overlap. As a result, we have shown that the second-order mixing parameter is appreciable and measurable. Indeed, it expresses the rate of intensity transferred between the overlapping lines A_1 and A_2 of each doublet. During this work, we have been able to show the line mixing effect on the line widths, which allows us to better understand the collisional dynamics of the molecules.

References

[1] Ridgway S. T., Wallace L., Smith G. R. The 800-1200 inverse centimeter absorption spectrum of Jupiter. *Astrophys. J.* 1976, 207, 1002-1006.

[2] Hanel R. A., Conrath B., Flasar M., Kunde V., Lowman P., Maguire W., Pearl J., Pirraglia J., Samuelson R. Infrared Observations of the Jovian System from Voyager 1. *Science.* 1979, 204, 972–976.

[3] Kunde V., Hanel R., Maguire W., Gautier D., Baluteau J. P., Marten A., Chedin A., Husson N., Scott N. The Tropospheric Gas Composition of Jupiter's North Equatorial Belt. (NH_3, PH_3, CH_3D, GeH_4, H_2O) and the Jovian D/H Isotopic Ratio. *Astrophys. J.* 1982, 263, 443–467.

[4] Larson H. P., Fink U., Smith H. A., Scott Davies D. The middle-infrared spectrum of Saturn: Evidence for phosphine and upper limits to other trace atmospheric constituents. *Astrophys. J.* 1980, 240, 327–337.

[5] Bouanich J. P., Salem J., Aroui H., Walrand J., Blanquet G. H_2-broadening coefficients in the ν_2 and ν_4 bands of PH_3. *J. Quant. Spectrosc. Radiat. Transf.* 2004, 84, 195-205.

[6] Salem J., Aroui H., Bouanich J. P., Walrand J., Blanquet G. Collisional broadening and line Intensities in the ν_2 and ν_4 bands of PH_3. *J. Mol. Spectrosc.* 2004, 225, 174-181.

[7] Salem J., Bouanich J. P., Walrand J., Aroui H., Blanquet G. Hydrogen line broadening in the ν_2 and ν_4 bands of phosphine at low temperature. *J. Mol. Spectrosc.* 2004, 228, 23-30.

[8] Salem J., Bouanich J. P., Walrand J., Aroui H., Blanquet G. Helium- and argon-broadening coefficients of phosphine lines in the ν_2 and ν_4 bands. *J. Mol. Spectrosc.* 2005, 232, 247-254.

[9] Bouanich J. P., Walrand J., Blanquet G. N_2-broadening coefficients in the ν_2 and ν_4 bands of PH_3. *J. Mol. Spectrosc.* 2005, 232, 40-46.

[10] Bouanich J. P., Blanquet G. N_2-broadening coefficients in the ν_2 and ν_4 bands of PH_3 at low temperature. *J. Mol. Spectrosc.* 2007, 241, 186-191.

[11] Salem J., Blanquet G., Lepère M., Aroui H. H_2 line mixing coefficients in the ν_2 and ν_4 bands of PH_3. *J. Mol. Spectrosc.* 2014, 297, 58-61.

[12] Salem J., Blanquet G., Lepère M., Aroui H. H_2 Line-mixing coefficients in the ν_2 and ν_4 bands of PH_3 at low temperature. *J. Quant. Spectrosc. Radiat. Transf.* 2016, 173, 34-39.

[13] Dufour G., Hurtmans D., Henry A., Valentin A., Lepère M. Line profile study from diode laser spectroscopy in the $^{12}CH_4$ $2\nu_3$ band perturbed by N_2, O_2, Ar, and He. *J. Mol. Spectrosc.* 2003, 221, 80-92.

[14] Maaroufi N., Kwabia Tchana F., Landsheere X., Aroui H. Pressure broadening and shift coefficients in the ν_1 and ν_3 bands of NH_3. *J. Quant. Spectrosc. Radiat. Transf.* 2018, 219, 383-392.

[15] Hmida F., Galalou S., Kwabia Tchana F., Rotger M., Aroui H. Line mixing effect in the ν_2 band of CH_3Br. *J. Quant. Spectrosc. Radiat. Transf.* 2017, 189, 351-360.

[16] Fissiaux L., Blanquet G., Lepère M. Diode-laser measurements of N_2-broadening coefficients in the ν_{10} band of allene at room temperature. *J. Quant. Spectrosc. Radiat. Transf.* 2012, 113, 1233-1239.

[17] Thibault F., Boissoles J., Le Doucen R., Farrenq R., Morillon-Chapey M., Boulet C. Line-by-line measurements of interference parameters for the 0–1 and 0–2 bands of CO in He, and comparison with coupled-states calculations. *J. Chem. Phys.* 1992, 97, 4623-4632.

[18] Salem J., Blanquet G., Lepère M., ben Younes R. H_2-broadening, shifting and mixing coefficients of the doublets in the ν_2 and ν_4 bands of PH_3 at room temperature. *Mol. Phys.* 2018, 116, 1280-1289.

[19] Smith E. W. Absorption and dispersion in the O_2 microwave spectrum at atmospheric pressures. *J. Chem. Phys.* 1981, 74, 6658-6673.

[20] Rosenkranz P. W. Shape of the 5 rnrn Oxygen Band in the Atmosphere. *IEEE. Trans. Antenn. Propag.* 1975, 23, 498-506.

[21] Baeten E., Blanquet G., Walrand J., Courtoy C. P. Tunable diode laser spectra of the ν_3-ν_1, region of CS_2. *Can. J. Phys.* 1984, 62, 1286-1292.

[22] Lepère M., Blanquet G., Walrand J., Bouanich J. P. Line intensities in the ν_6 band of CH_3F at 8.5 μm. *J. Mol. Spectrosc.* 1996, 180, 218-226.

[23] Hitran Data Bases. http://www.hitran.org/results/5a1856e6.par

[24] Press W. H., Flannery B. P., Tendolsky S. A., Vetterling W. T. Numerical Recipes−The Art of Scientific Computing (FORTRAN Version). *Cambridge Univ. Press, Cambridge,* 1992.

[25] Blanquet G., Walrand J., Bouanich J. P. Diode-Laser Measurements of O_2-Broadening Coefficients in the ν_3 band of $CH_3{}^{35}Cl$. *J. Mol. Spectrosc.* 1993, 159, 137-143.

[26] Humlíček J. An efficient method for evaluation of the complex probability function: The Voigt function and its derivatives. *J. Quant. Spectrosc. Radiat. Transf.* 1979, 21, 309-313.

[27] Pine A. S. Line mixing sum rules for the analysis of multiplet spectra. *J. Quant. Spectrosc. Radiat. Transf.* 1997, 57, 145-155.

[28] Brown L. R., Sams R. L., Kleiner I., Cottaz C., Sagui L. Line Intensities of the Phosphine Dyad at 10 μm. *J. Mol. Spectrosc.* 2002, 215, 178-203.

[29] Devi V. M., Benner D. C., Kleiner I., Sams R. L., Fletcher L. N. Line shape parameters of PH_3 transitions in the Pentad near 4–5 μm: Self-broadened widths, shifts, line mixing and speed dependence. *J. Mol. Spectrosc.* 2014, 302, 17-33.